

Self-Assembly of Alkali-Uranyl-Peroxide Clusters

May Nyman* and Mark A. Rodriguez

Sandia National Laboratories Albuquerque, New Mexico 87185

Charles F. Campana

Bruker AXS Inc. Madison, Wisconsin 53711

Received March 18, 2010

The hexavalent uranium specie, uranyl triperoxide, $\text{UO}_2(\text{O}_2)_3^{4-}$, has been shown recently to behave like high oxidation-state d^0 transition-metals, self-assembling into polyoxometalate-like clusters that contain up to 60 uranyl cations bridged by peroxide ligands. There has been much less focus on synthesis and structural characterization of salts of the monomeric $\text{UO}_2(\text{O}_2)_3^{4-}$ building block of these clusters. However, these could serve as water-soluble uranyl precursors for both clusters and materials, and also be used as simple models to study aqueous behavior by experiment and modeling. The counteranion is of utmost importance to the assembly of these clusters, and Li^+ has proven useful for the crystallization of many of the known cluster geometries to date. We present in this paper synthesis and structural characterization of two monomeric lithium uranyl-peroxide salts, $\text{Li}_4[\text{UO}_2(\text{O}_2)_3] \cdot 10\text{H}_2\text{O}$ (**1**) and $[\text{UO}_2(\text{O}_2)_3]_{12}[\text{UO}_2(\text{OH})_4]\text{Li}_{16}(\text{H}_2\text{O})_{28}]_3 \cdot \text{Li}_6[\text{H}_2\text{O}]_{26}$ (**2**). They were obtained from aqueous-alcohol solutions rather than the analogous aqueous solutions from which lithium uranyl-peroxide clusters are crystallized. Rapid introduction of the alcohol gives the structure of (**1**) whereas slow diffusion of alcohol results in crystallization of (**2**). (**2**) is an unusual structure featuring uranyl-centered alkali clusters that are linked into ring and spherical arrangements via $[\text{UO}_2(\text{O}_2)_3]$ anions. Furthermore, partial substitution of Rb or Cs into the synthesis results in formation of (**2**) with substitution of these larger alkalis into the uranyl-centered clusters. We surmise that the slow crystallization allows for direct bonding of alkali metals to the uranyl-peroxide oxygen ligands that is observed in (**2**), and its Rb and Cs-substituted derivatives. In contrast, the only interaction between $\text{UO}_2(\text{O}_2)_3^{4-}$ and Li^+ observed in (**1**) is through hydrogen bonding of the lithium-bound water. These structures potentially provide some insight to understanding how alkali counterions interact with the $\text{UO}_2(\text{O}_2)_3^{4-}$ anions during the self-assembly, crystallization and even redissolution of uranyl-peroxide polyanionic clusters.

Introduction

The aqueous^{1–3} and solid-state⁴ chemistries of the uranyl cation U(VI)O_2^{2+} are incredibly versatile. The oxo, or “yl” oxygens define an $\text{O}=\text{U}=\text{O}$ axis, perpendicular to which there are generally four to six bonds to uranium in the equatorial plane, resulting in square-bipyramid, pentagonal-bipyramid or hexagonal-bipyramid geometry. U(VI)O_2^{2+} is soluble in both alkaline and acidic aqueous solutions, as either an anion or a cation, depending on its equatorial ligands. There particularly has been much recent focus on the solid-state

chemistry of the triperoxo-uranyl anion, $\text{UO}_2(\text{O}_2)_3^{4-}$. Peroxide is well-known in its ability to dissolve UO_2 fuel pellets in carbonate-rich (alkaline) solutions, by both oxidizing and ligating the uranium.^{5,6} Studtite, a uranium-peroxo mineral forms in nature and on the surface of fuel pellets, where the only source of peroxide is radiolysis of water, illustrating the incredible stability of the bidentate bond that peroxide forms with U(VI) .^{7,8} The triperoxo-uranyl anion crystallizes with hydrated counter-cations,^{9–11} or self-assembles into a variety

*To whom correspondence should be addressed. E-mail: mdnyman@sandia.gov.

(1) Szabo, Z.; Toraiishi, T.; Vallet, V.; Grenthe, I. *Coord. Chem. Rev.* **2006**, *250*, 784–815.

(2) DenAuwer, C.; Simoni, E.; Conradson, S.; Madic, C. *Eur. J. Inorg. Chem.* **2003**, *21*, 3843–3859.

(3) Clark, D. L.; Conradson, S. D.; Donohoe, R. J.; Keogh, D. W.; Morris, D. E.; Palmer, P. D.; Rogers, R. D.; Tait, C. D. *Inorg. Chem.* **1999**, *38*, 1456–1466.

(4) Burns, P. C.; Ewing, R. C.; Hawthorne, F. C. *Canad. Miner.* **1997**, *35*, 1551–1570.

(5) Peper, S. M.; Brodnax, L. F.; Field, S. E.; Zehnder, R. A.; Valdez, S. N.; Runde, W. H. *Ind. Eng. Chem. Res.* **2004**, *43*, 8188–8193.

(6) Kim, K. W.; Kim, Y. H.; Lee, S. Y.; Lee, J. W.; Joe, K. S.; Lee, E. H.; Kim, J. S.; Song, K.; Song, K. C. *Environ. Sci. Technol.* **2009**, *43*, 2355–2361.

(7) Kubatko, K. A.; Helean, K. B.; Navrotsky, A.; Burns, P. C. *Science* **2003**, *302*, 1191–1193.

(8) Hughes, K. A.; Burns, P. C. *Am. Mineral.* **2003**, *88*, 1165–1168.

(9) Alcock, N. W. *J. Chem. Soc. A* **1968**, 1588–1594.

(10) Kubatko, K. A.; Forbes, T. Z.; Klingensmith, A. L.; Burns, P. C. *Inorg. Chem.* **2007**, *46*, 3657–3662.

(11) Zehnder, R. A.; Batista, E. R.; Scott, B. L.; Peper, S. M.; Goff, G. S.; Runde, W. H. *Radiochim. Acta* **2008**, *96*, 575–578.

of uranyl-peroxide polyanions that range in nuclearity from small clusters,^{12,13} rings and crowns,¹⁴ to nanospheres containing up to 60 uranium atoms.^{15–18} Since the report of the first uranyl (and neptunyl) peroxide polynuclear clusters in 2005,¹⁶ the class of compounds has grown rapidly, suggesting there is much more aqueous and solid-state uranyl-peroxide chemistry yet to be discovered.

Most often the many polynuclear species reported in recent years by Burns et al. are crystallized from aqueous solutions that are very high in hydroxide, peroxide, and uranyl concentration. On the other hand, the Na, Ca, and Na/Rb salts^{9,10} of monomeric $[\text{UO}_2(\text{O}_2)_3]^{4+}$ were obtained by introducing a less polar “non-solvent” to the aqueous solution. These monomeric $[\text{UO}_2(\text{O}_2)_3]^{4+}$ salts are important because they can potentially be exploited as precursors for the synthesis of novel cluster topologies or framework materials, providing another avenue for expanding this field of chemistry. Furthermore, they are useful as simple models for experimental and computational studies of aqueous and solid-state behavior of uranyl-peroxides. With these goals in mind, we are currently exploring crystallization of water-soluble uranyl complexes with a variety of counter-cations from mixed water–alcohol media.

Lithium has proved a very important counterion in developing uranyl-peroxide cluster chemistry, resulting in the crystallization of clusters containing 24, 28, 30, 32, 36, 40, 44, 50, and 60 $\text{UO}_2(\text{O}_2)_3$ units.^{15–18} Additionally, the lithium counterion provides the best solubility for various cluster sizes and geometries; much like acidic polyoxometalates, polyoxotungstates in particular.¹⁹ For both uranyl-peroxide clusters and the polyoxotungstate clusters, addition of lithium salt in excess results in aqueous dissolution of otherwise insoluble compounds and renders aqueous phase studies possible. Despite the importance of lithium to both solution and solid-state chemistry of the uranyl-peroxide clusters, lithium salts of monomeric uranyl triperoxide have not been structurally characterized. We report here the crystallization and structural studies of two new lithium uranyl salts from aqueous-alcohol mixtures. By rapid addition of alcohol, we obtain $\text{Li}_4[\text{UO}_2(\text{O}_2)_3] \cdot 10\text{H}_2\text{O}$, which has features in common with both Alcock's and Burns' sodium uranyl triperoxide salts.^{9,10} However, if the alcohol is introduced by vapor diffusion, an unusual and complex structure, $[\text{UO}_2(\text{O}_2)_3]_{12}[(\text{UO}_2(\text{OH})_4)\text{Li}_{16}(\text{H}_2\text{O})_{28}]_3 \cdot \text{Li}_6[\text{H}_2\text{O}]_{26}$, is obtained. This structure features two different uranyl coordination environments; and one uranyl sits in the center of a polyoxometalate-like clusters containing 16 Li^+ polyhedra, and these are linked together by $[\text{UO}_2(\text{O}_2)_3]^{4-}$ anions into a spherical arrangement. Self-assembly

of this latter structure appears to be a product ion-pairing interactions between lithium cations and uranyl-peroxide and uranyl-hydroxyl anions. This same arrangement of alkali-uranyl clusters linked into rings and then spheres is also observed with partial substitution of Rb^+ or Cs^+ into the cluster, if Rb or Cs salts are included as minor alkali components of the synthesis solution.

Synthesis

$\text{Li}_4[\text{UO}_2(\text{O}_2)_3] \cdot 10\text{H}_2\text{O}$ (1) Part A. A small beaker (40 mL) was placed in an ice bath with a stir bar. Twelve milliliters of DI water, 6 mL of 30% H_2O_2 aqueous solution, 8 mL of 4 M LiOH solution, and 1 g of $\text{UO}_2(\text{NO}_3)_2 \cdot 6\text{H}_2\text{O}$ were combined in the beaker. Rapid stirring resulted in a clear yellow solution. The final solution concentration was 0.815 M LiOH, 6.9% H_2O_2 , 0.077 molar UO_2^{2+} . Rapid addition of ~ 30 mL of alcohol (methanol, ethanol, or isopropanol) to the aqueous solution resulted in precipitation of a yellow crystalline solid, which was isolated by vacuum filtration. The filtrate was nearly colorless, and the yield was 2.2 g (96% yield).

$[\text{UO}_2(\text{O}_2)_3]_{12}[(\text{UO}_2(\text{OH})_4)\text{Li}_{16}(\text{H}_2\text{O})_{28}]_3 \cdot \text{Li}_6[\text{H}_2\text{O}]_{26}$ (2) Part A. The same procedure described above was executed. However, rather than rapid addition of alcohol, it was diffused in slowly. This was achieved by placing the beaker inside a larger jar containing enough alcohol to cover ~ 1 in. of the bottom of the jar, and the jar was capped. Well-formed yellow crystals with a dodecahedral shape grew on the bottom and sides of the beaker after several days. The yield ranged from ~ 1.0 – 1.5 g, approximately 50–75% yield, depending on how long the reaction was left to crystallize. This process was carried out at room temperature.

Synthesis of (2) with substitution of Rb^+ and Cs^+ . Lithium hydroxide (1.34 g $\text{LiOH} \cdot \text{H}_2\text{O}$, 32 mmol) and either 0.12 g of RbCl or 0.17 g of CsCl (both 1 mmol) was dissolved in 10 mL of DI H_2O . Aqueous hydrogen peroxide (3 mL 30% H_2O_2) was added, and the resulting solution was placed in a 50 mL beaker in an ice bath. Uranyl nitrate hexahydrate (0.1 g, 0.2 mmol) was added to the cooled solution, resulting in a yellow-orange clear solution. The beaker containing the solution was then set inside a larger jar containing approximately one inch of ethanol, and the jar was capped. After approximately one week of diffusion of ethanol (~ 3 mL) into the aqueous solution, large, well-formed yellow cubes were observed. The diffusion process took place at room temperature. These were isolated into oil for single-crystal X-ray diffraction.

Synthesis of (1) and (2) Part B. Uranyl-peroxide-LiOH solutions were prepared following the procedure for the U_{24} nanosphere reported by Burns et al.¹⁶ Briefly, 30% H_2O_2 (5 mL), H_2O (1 mL), $\text{LiOH} \cdot \text{H}_2\text{O}$ (1 g), and 2 M $[\text{UO}_2(\text{NO}_3)_2 \cdot 6\text{H}_2\text{O}]$ solution in H_2O (1 mL) was placed in a 40 mL beaker inside an icebath, and dissolution of the uranyl salt was accomplished by rapid stirring. The final solution was 0.29 molar UO_2^{2+} (1.0 g) 21% H_2O_2 , and 3.4 M LiOH. Slow diffusion of methanol produced a large crop of crystals, a mixture of (1) and (2) overnight, and rapid addition of alcohol followed by vacuum filtration gave a batch of (1).

Single Crystal X-ray Diffraction. Single-crystal X-ray diffraction of (1), (2), Cs-(2a), and Cs-(2b) were performed at 100 K on a Bruker AXS SMART-CCD diffractometer

(12) Sigmon, G. E.; Ling, J.; Unruh, D. K.; Moore-Shay, L.; Ward, M.; Weaver, B.; Burns, P. C. *J. Am. Chem. Soc.* **2009**, *131*, 16648–16649.

(13) Unruh, D. K.; Burtner, A.; Burns, P. C. *Inorg. Chem.* **2009**, *48*, 2346–2348.

(14) Sigmon, G. E.; Weaver, B.; Kubatko, K. A.; Burns, P. C. *Inorg. Chem.* **2009**, *48*, 10907–10909.

(15) Sigmon, G. E.; Unruh, D. K.; Ling, J.; Weaver, B.; Ward, M.; Pressprich, L.; Simonetti, A.; Burns, P. C. *Angew. Chem., Int. Ed.* **2009**, *48*, 2737–2740.

(16) Burns, P. C.; Kubatko, K. A.; Sigmon, G.; Fryer, B. J.; Gagnon, J. E.; Antonio, M. R.; Soderholm, L. *Angew. Chem., Int. Ed.* **2005**, *44*, 2135–2139.

(17) Forbes, T. Z.; McAlpin, J. G.; Murphy, R.; Burns, P. C. *Angew. Chem., Int. Ed.* **2008**, *47*, 2824–2827.

(18) Unruh, D. K.; Burtner, A.; Pressprich, L.; Sigmon, G. E.; Burns, P. C. *Dalton Trans.* **2010**, *39*, 5807–5813.

(19) Acerete, R.; Hammer, C. F.; Baker, L. C. W. *J. Am. Chem. Soc.* **1982**, *104*, 5384–5390.

Table 1. Crystallographic Information for (1) and (2)

	(1) $\text{Li}_4[\text{UO}_2(\text{O}_2)_3] \cdot 10\text{H}_2\text{O}$	(2) $[\text{UO}_2(\text{O}_2)_3]_{12} \cdot [(\text{UO}_2(\text{OH})_4)\text{Li}_{16}(\text{H}_2\text{O})_{28}]_3 \cdot \text{Li}_6[\text{H}_2\text{O}]_6$
formula	$\text{H}_{20}\text{O}_{18}\text{Li}_4\text{U}$	$\text{H}_{232}\text{O}_{224}\text{Li}_{54}\text{U}_{15}$
formula weight	574	7759
crystal system	orthorhombic	cubic
space group	<i>Pbcn</i> (no. 60)	<i>Pm</i> $\bar{3}$ <i>m</i> (no. 221)
<i>a</i> (Å)	13.1179(14)	17.4598 (11)
<i>b</i> (Å)	9.2359(10)	17.4598 (11)
<i>c</i> (Å)	12.8958(14)	17.4598 (11)
volume (Å ³)	1562.40(29)	5322.53(58)
<i>Z</i>	4	12
<i>d</i> _{calc} (g/cm ³)	2.440	2.327
min/max θ [deg]	2.70/26.39	1.17/23.28
final R_1^a [$I > 2\sigma(I)$]	0.0153	0.0352
final wR_2^b [$I > 2\sigma(I)$]	0.0335	0.1227
GO _F	1.061	1.278

$$^a R_1 = \sum ||F_o| - |F_c|| / \sum |F_o|. \quad ^b wR_2 = \{ \sum w(F_o^2 - F_c^2)^2 / \sum w(F_o^2)^2 \}^{0.5}$$

with graphite monochromated Mo K α (0.71073 Å) radiation. Data collection and reduction were carried out with SMART 5.054 (Bruker, 1998) and SAINT 6.02 (Bruker, 2001) software, respectively. Empirical absorption correction was applied using SADABS. All subsequent structure solution and refinement were performed within the WinGX system. The structures were solved by Direct Methods (program SIR97) and refined by full matrix least-squares on F^2 (SHELX97). While (2) and Cs-(2a) were solved in the *Pm* $\bar{3}$ *m* space group with $a \sim 17.5$ Å, Cs-(2b) was solved and refined in the space group *Im* $\bar{3}$ with an approximate doubled unit cell of $a \sim 35$ Å. Furthermore, the crystal was identified as a perfect merohedral twin (with equal scattering from each component) with a twin law of 0 1 0 1 0 0 0 -1.

Characterization Techniques. In addition to single-crystal X-ray diffraction, (1) and (2) were also characterized by powder X-ray diffraction and infrared spectroscopy. X-ray powder diffraction was carried out on a Bruker D8 Advance diffractometer in Bragg–Brentano geometry with Cu–K α radiation and a diffracted-beam graphite monochromator. Fourier transform infrared (FTIR) spectra were collected on a PerkinElmer Spectrum One instrument. Powders of uranyl salts were mixed into KBr matrix and pressed into pellets for analysis.

Results and Discussion

Structure Descriptions. Crystallographic data for (1) and (2) are summarized in Table 1. Tables 2 and 3 respectively summarize pertinent bond lengths (discussed below) and bond valence sum values for (1) and (2). The BVS values range from 6.2–6.6 for the two structures. These are a little bit higher than expected for U⁶⁺. However, this is a common trend observed for f-electron actinides,⁴ which generally deviate from the empirically derived equation for BVS calculations.²⁰ The equation we utilized for BVS calculations is

$$\text{BVS} = \exp((2.045 - \text{BL})/0.519)); \quad \text{BL} = \text{bond length in angstroms} \quad (1)$$

Table 2. U–O Bond Lengths and Bond Valence Sum (BVS)^a for $\text{Li}_4[\text{UO}_2(\text{O}_2)_3] \cdot 10\text{H}_2\text{O}$ (1)

atom1	atom2	bond length (Å)	bond valence of U–O bond
U1	O3	1.846(2)	1.467
	O3	1.846(2)	1.467
	O1	2.303(2)	0.608
	O1	2.303(2)	0.608
	O9	2.322(2)	0.586
	O9	2.322(2)	0.586
	O4	2.324(2)	0.584
	O4	2.324(2)	0.584
Total BVS of U1			6.492

^a Using values from P.C. Burns et al., 1997.⁴ See also eq 1 in text.

Table 3. Pertinent Bond Lengths and Bond Valence Sums (BVS)^a for $[\text{UO}_2(\text{O}_2)_3]_{12}[(\text{UO}_2(\text{OH})_4)\text{Li}_{16}(\text{H}_2\text{O})_{28}]_3 \cdot \text{Li}_6[\text{H}_2\text{O}]_6$ (2)

atom 1	atom 2	bond length (Å)	BVS
U1 $[\text{UO}_2(\text{O}_2)_3]$ (linking clusters)	O3	1.847(9)	1.464
	O3	1.847(9)	1.464
	O2	2.28 (1)	0.638
	O2	2.28 (1)	0.638
	O4	2.30 (1)	0.612
	O4	2.30 (1)	0.612
	O1	2.32 (1)	0.586
	O1	2.32 (1)	0.586
Total BVS of U1			6.602
U2 $[\text{UO}_2(\text{OH})_4]$ (center of cluster)	O8	1.76 (5)	1.748
	O8	1.76(5)	1.748
	O9	2.25 (3)	0.671
	O9	2.25 (3)	0.671
	O9	2.25 (3)	0.671
	O9	2.25 (3)	0.671
Total BVS of U2			6.18
O9 (OH)	L12	2.09 (4)	0.202
	L12	2.09 (4)	0.202
	L13	2.17 (5)	0.163
	U2	1.76 (5)	0.671
Total BVS of O9 (without H)			1.238

^a Using values from P.C. Burns et al., 1997.⁴ See also eq 1 in text.

$\text{Li}_4[\text{UO}_2(\text{O}_2)_3] \cdot 10\text{H}_2\text{O}$ (1). The $[\text{UO}_2(\text{O}_2)_3]^{4-}$ hexagonal bipyramidal monomer has typical U=O bonds around 1.8 Å, and the U–O bonds between uranium and the peroxide ligand are around 2.3 Å. (see Table 2). Each lithium cation is in tetrahedral coordination, bonded to four water molecules with Li–O distances ranging from 1.9 to 2.0 Å. The $\text{Li}(\text{H}_2\text{O})_4$ tetrahedra are corner and edge sharing, forming rings of eight lithium tetrahedra in the *xy* plane (Figure 1). The $[\text{UO}_2(\text{O}_2)_3]^{4-}$ anions form layers between the Li–H₂O layers, where a single monomer is sandwiched in the center of two $\text{Li}^+ - \text{H}_2\text{O}$ rings (Figure 2). Both the “yl” and the peroxo oxygens are H-bonded to the water molecules with H---O distances ranging from 2.1 to 2.9 Å. This structure has features in common with the structure of $\text{Na}_4[\text{UO}_2(\text{O}_2)_3] \cdot 9\text{H}_2\text{O}$ reported by Alcock et al.⁹ The sodium salt also has layers of rings of corner and edge sharing Na–H₂O polyhedra. However, the sodium also coordinates directly to the yl oxygens of the $\text{UO}_2(\text{O}_2)_3$ anion. A similar sodium triperoxo-uranyl salt, $\text{Na}_4[\text{UO}_2(\text{O}_2)_3] \cdot 12\text{H}_2\text{O}$ was reported in 2007¹⁰ that features the same alternating layers of $\text{UO}_2(\text{O}_2)_3$ and Na–water layers, only interacting through H-bonding of the water to the yl oxygens.

$[\text{UO}_2(\text{O}_2)_3]_{12}[(\text{UO}_2(\text{OH})_4)\text{Li}_{16}(\text{H}_2\text{O})_{28}]_3 \cdot \text{Li}_6[\text{H}_2\text{O}]_{26}$ (2). This lithium uranyl phase contains two uranyl coordination

(20) Brese, N. E.; O’Keefe, M. *Acta Crystallogr., Sect. B* 1991, 47, 192–197.

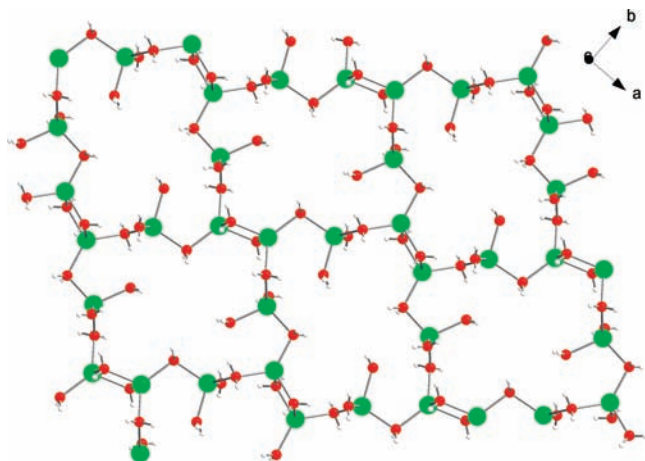


Figure 1. View down the *c*-axis of $\text{Li}_4[\text{UO}_2(\text{O}_2)_3] \cdot 10\text{H}_2\text{O}$ (1) of the Lithium-water layers. Red spheres are oxygen, green spheres are lithium, and white spheres are hydrogen.

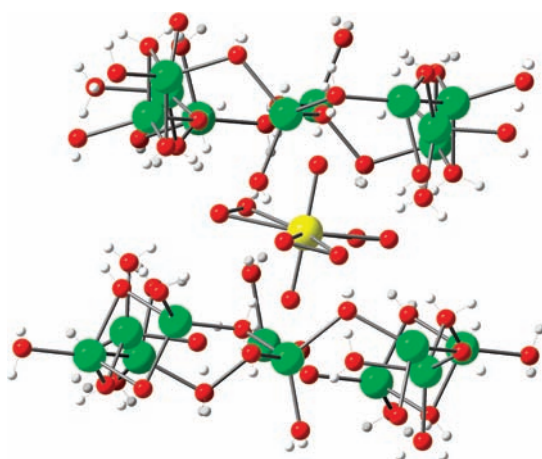


Figure 2. View of the $\text{UO}_2(\text{O}_2)_3^{4-}$ specie of (1), between two lithium-water layers. The yellow sphere is uranium, red spheres are oxygen, green spheres are lithium, and white spheres are hydrogen.

geometries. U1 is the $\text{UO}_2[\text{O}_2]_3^{4-}$ geometry. We have deduced U2 to be octahedrally coordinated, $\text{UO}_2(\text{OH})_4^{2-}$. In the equatorial plane of U2 (perpendicular to the UO_2 axis), there are 8 oxygen (O9) atoms. Two O9 atoms are 1.38 Å apart and the U2–O9 bond is 2.25 Å, both reasonable distances for a Uranyl-bonded peroxy-ligand. However, the large thermal parameters of O9 suggested partial occupancy; and decreasing the occupancy of this site to 1/2 gave more reasonable values, which would result in an octahedrally coordinated U2. The bond valence of O9 is 1.24, suggesting it requires a proton, which also helps satisfy charge-balance requirements, and the geometry of O9 is reasonable to bond a proton. Therefore we have designated O9 a hydroxyl, although we cannot locate the proton, likely because of much disorder in this structure, and the H's proximity to heavy uranium atoms. This coordination geometry, $[\text{UO}_2(\text{OH})_4]^{2-}$ has been reported prior for $[\text{Co}(\text{NH}_3)_6]_2[\text{UO}_2(\text{OH})_4] \cdot 3\text{H}_2\text{O}$.³

U2 sits at the center of what may be described as a lithium-uranyl polyoxometalate-like cluster, which is shown in Figure 3. The “cluster” is formulated $[\text{UO}_2(\text{OH})_4\text{Li}_{16}\text{O}_8(\text{H}_2\text{O})_{28}]^{2-}$ (ULi_{16}). The Li^+ cations are in square-pyramidal or distorted octahedral coordination with Li–O

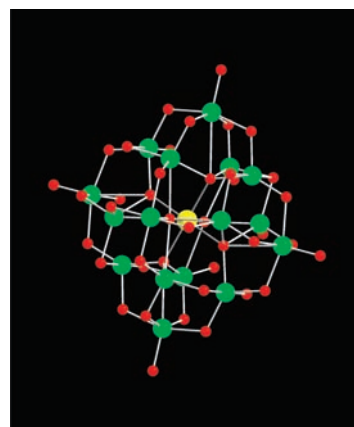


Figure 3. View of (2) showing the $[\text{UO}_2(\text{OH})_4\text{Li}_{16}\text{O}_8(\text{H}_2\text{O})_{28}]$ cluster. The yellow sphere is uranium, red spheres are oxygen, and green spheres are lithium.

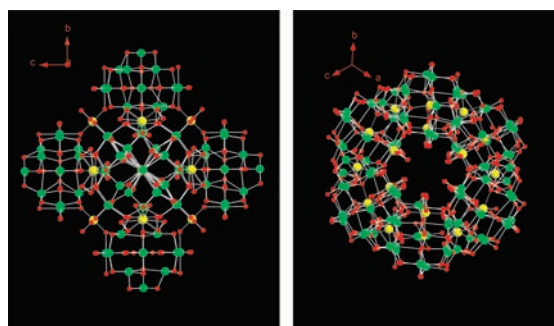


Figure 4. (a; left) View of (2) down the *a*-axis showing four ULi_{16} clusters joined in a ring by four $[\text{UO}_2(\text{O}_2)_3]^{4-}$. (b; right) View down the (111) axis showing three ULi_{16} linked by three $[\text{UO}_2(\text{O}_2)_3]^{4-}$. The yellow spheres are uranium, red spheres are oxygen, and green spheres are lithium.

bonds between 1.9 and 2.2 Å; and the Li and U polyhedra are edge-sharing. The eight O^{2-} ligands within ULi_{16} are the “y1” oxygens of U1 $[\text{UO}_2(\text{O}_2)_3]^{4-}$; thus each U2-centered cluster links to eight U1 $[\text{UO}_2(\text{O}_2)_3]^{4-}$, and each U1 bridges two of the ULi_{16} clusters through its oxo-ligands. Lithium has been observed before to assemble with water and oxo ligands as clusters in alkaline aqueous solution. For instance, the lithium salt of $[\text{Nb}_6\text{O}_{19}]^{8-}$ polyoxometalate features adamantane-like clusters of lithium, water, and oxo ligands from the $[\text{Nb}_6\text{O}_{19}]^{8-}$ cluster.²¹

When viewed down the *a*, *b*, or *c*-axes, four ULi_{16} clusters are linked by four $[\text{UO}_2(\text{O}_2)_3]^{4-}$ bridges to form a window composed of four ULi_{16} clusters and bridged by four $[\text{UO}_2(\text{O}_2)_3]^{4-}$ anions (Figure 4a). The view down the (111) axis reveals a window composed of three ULi_{16} clusters bridged by three $[\text{UO}_2(\text{O}_2)_3]^{4-}$ anions. By viewing only the $[\text{UO}_2(\text{O}_2)_3]^{4-}$ and $[\text{UO}_2(\text{OH})_4]^{2-}$ anions within a sphere, or the unit cell (Figure 5), we observe they are arranged in a spherical fashion, with the $[\text{UO}_2(\text{OH})_4]^{2-}$ located on each face of the unit cell (total of 6) and twelve $[\text{UO}_2(\text{O}_2)_3]^{4-}$. In the center of this sphere are disordered water molecules that are hydrogen-bonded to one another (O11; O11–O11 distance ~ 2.5 Å). O12 is also lattice water that is only associated by H-bonding to water

(21) Anderson, T. M.; Thoma, S. G.; Bonhomme, F.; Rodriguez, M. A.; Park, H.; Parise, J. B.; Alam, T. M.; Larentzos, J. P.; Nyman, M. *Cryst. Growth Des.* **2007**, *7*, 719–723.

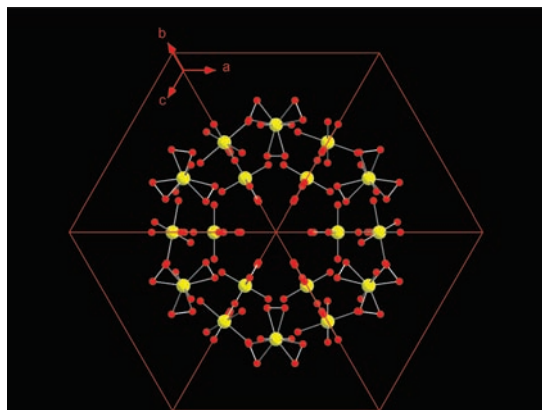


Figure 5. View of the unit cell of **(2)** down the (111) direction, observing only the uranyl polyhedra. In the center (not shown) is a cube of disordered water. The $\text{UO}_2(\text{OH})_4^{2-}$ occupy each face of the cubic unit cell, and there are 12 $\text{UO}_2(\text{O}_2)_3^{4-}$ anions within the unit cell.

molecules (O–O distance ~ 2.6 Å) and peroxo-ligands (O–O distance ~ 2.9 Å). Near the corner of the unit cell (close to (0,0,0)) there are disordered waters and lithium that fill the space between these spherical aggregates of ULi_{16} clusters: a total of 6 Li^+ and 26 H_2O in the unit cell. Initially in the refinement, we ignored these electron density peaks. However, if they are left out of the structural refinement, solvent-accessible void space is identified. Furthermore, by including these atoms, the *R*-factor decreases by $\sim 0.4\%$, and charge-balance is achieved. Considering only the uranyl anions (Figure 5), the structure of **(2)** has some commonalities with the nanospheres such as U_{24} ¹⁶ and the fullerene¹⁷ topologies. The uranyl anions take on a spherical arrangement, like the nanospheres. Furthermore, the center of the “sphere” of **(2)** and the centers of many of these nanospheres are crystallographically challenging, containing disordered alkalis, water, and even a partially occupied uranyl, in the case of U_{28} .¹⁶ These similarities might suggest that alkali counterions play a role in defining the spherical topology of the uranyl peroxide nanospheres, in addition to the influence of the bent O=U=O angle.

Partial Substitution of Rb or Cs into (2). Multiple single-crystal X-ray diffraction data sets were collected on the well-formed yellow cube-shaped crystals of **(2)** that were crystallized from the mixed Rb–Li– $[\text{UO}_2(\text{O}_2)_3]$ or Cs–Li– $[\text{UO}_2(\text{O}_2)_3]$ precursor solids. The presence of Rb or Cs was confirmed by energy dispersive spectroscopy. The *a*-parameter, cell volume, and space group of two Cs–Li phases are summarized in Table 4, and also compared to that of **(2)**. Although we have determined unit cells and partial solutions from single-crystals extracted from other syntheses (both Rb and Cs substituted), we only present these two structures listed in Table 4, **Cs-(2a)** and **Cs-(2b)** because of the difficulty in obtaining completed satisfactory solutions. Problems with these structures are described below, as well as in the experimental section. In every case, with substitution of Rb or Cs, the *a*-dimension and volume are respectively ~ 0.10 – 0.15 Å and ~ 300 Å³ larger than without Rb or Cs substitution. In some cases, a doubled unit cell was measured, as is the case for **Cs-(2b)**. However, the same cell was never measured twice, which suggests each batch of crystals had different ratios of Li/Cs; with Cs/Rb substituting for Li both within the

clusters and interstitial to the clusters. Furthermore, zoned crystals are a possibility, with varying Li/Rb or Li/Cs ratio from the center to the edge of a single-crystal. This cubic lattice appears very flexible, accommodating disorder and substitution of disparate ion sizes (i.e., Li vs Cs).

The disorder, partial occupancies, and mixed occupancies in the Cs-substituted structures imparted some difficulties with optimizing the structural refinements. This is particularly true in the “intercluster” regions of the structure. In particular, for **Cs-(2b)**, some O atoms on peroxo ligands show skewing resulting in $U_{\text{eq_max/min}}$ values that were significantly distorted. This was attempted to be modeled as dual partial site occupancy, but the refinement showed highly correlated atoms and additional issues with atomic displacement parameters. Thus, the O atoms were left as single site locations with distorted ellipsoids. Also, the twinned structure may have impacted integration results, thereby causing possible unexpected distortion of atomic displacement parameters. The inability to locate water hydrogens probably also contributed to elongation of thermal ellipsoids. **Cs-(2b)** contained solvent accessible voids of 230 Å³. Attempts to model all possible solvent atoms were made and all possible large Q peaks were checked for missed solvent. It was concluded that the remaining large Q peaks (> 2.5) were associated with truncation errors around U or Cs atoms and not associated with significant missed solvent.

However, despite these issues, the structures of **Cs-(2a)** and **Cs-(2b)** were of acceptable resolution to provide information of how the larger alkalis substitute for Li within the uranyl-alkali clusters. All of the structures contain a uranyl sitting in the center of 10–18 alkali polyhedra, and these clusters are decorated by eight $\text{UO}_2(\text{O}_2)_3^{4-}$ anions that link the uranyl-alkali clusters into rings and spheres. Figure 6 shows both the clusters and the linkage of four clusters into a ring via four $[\text{UO}_2(\text{O}_2)_3]^{4-}$ anions for **Cs-(2a)** and **Cs-(2b)**. Like in **(2)**, the central uranyl for **Cs-(2a)** is best described as octahedrally coordinated $[\text{UO}_2(\text{OH})_4]^{2-}$, which also accommodates charge-balance. Again, the H's are not located, and the four OH[−] ligands are 8 half-occupied sites. **Cs-(2a)**, on the other hand features a $[\text{UO}_2(\text{O}_2)_3]^{4-}$ anion in the center of the cluster. The uranyl-centered clusters for **Cs-(2a)** and **Cs-(2b)** are respectively best formulated as $[[\text{UO}_2(\text{OH})_4]\text{Cs}_4\text{Li}_6(\text{H}_2\text{O})_{24}]^{8+}$ and $[[\text{UO}_2(\text{O}_2)_3]\text{Cs}_2\text{Li}_{10}(\text{H}_2\text{O})_{19}]^{8+}$. The Cs–O distances of the Cs that sits within the uranyl-centered cluster for **Cs-(2a)** range from 2.89 to 3.60(1) Å, and the Cs is 11-coordinate. Like in the structure of **(2)**, the Li–O distances range from 1.91 to 2.21(1) Å, and lithium polyhedra are square pyramidal or distorted octahedral. Similarly, the Cs within the cluster of **Cs-(2b)** is 12-coordinate with Cs–O distances from 3.07 to 3.66(1) Å, and similar Li–O distances and coordination geometries. Finally, in **Cs-(2a)**, a $[\text{Li}_{24}(\text{H}_2\text{O})_{12}(\text{O}_2)_{24}]$ cluster sits in the corner of the unit-cell (centered on the origin), linking the spheres of uranyl-linked alkali-uranyl clusters (Figure 7).

Infrared Spectra of (1) and (2). The infrared spectra from 400 to 2000 cm^{-1} of **(1)**, **(2)**, and also $\text{Na}_4[\text{UO}_2(\text{O}_2)_3] \cdot 9\text{H}_2\text{O}$ (for comparison) are shown in Figure 8. The overlapping bands in the region of 600–900 cm^{-1} have been previously identified as the vibrations of both the UO_2 unit and the U-peroxide bonds.⁹ Therefore the broad

Table 4. Comparing Unit Cells for Analogues of (2)

alkali	space group	a (Å)	volume (Å ³)	comments on structure refinement
Li only (2)	$Pm\bar{3}m$	17.4598 (11)	5322.53	good refinement, down to $R_1 = 3.5\%$
Cs–Li Cs-(2a)	$Pm\bar{3}m$	17.548 (2)	5403.23	acceptable refinement, down to $R_1 = 9.3\%$
Cs–Li Cs-(2b)	$Im\bar{3}$	35.0945 (18) [17.5472] ^a	43223.43 [5402.90] ^a	acceptable refinement down to $R_1 = 6.3\%$

^a $a/2$ or $a^3/8$ for direct size comparison to the related half-cells.

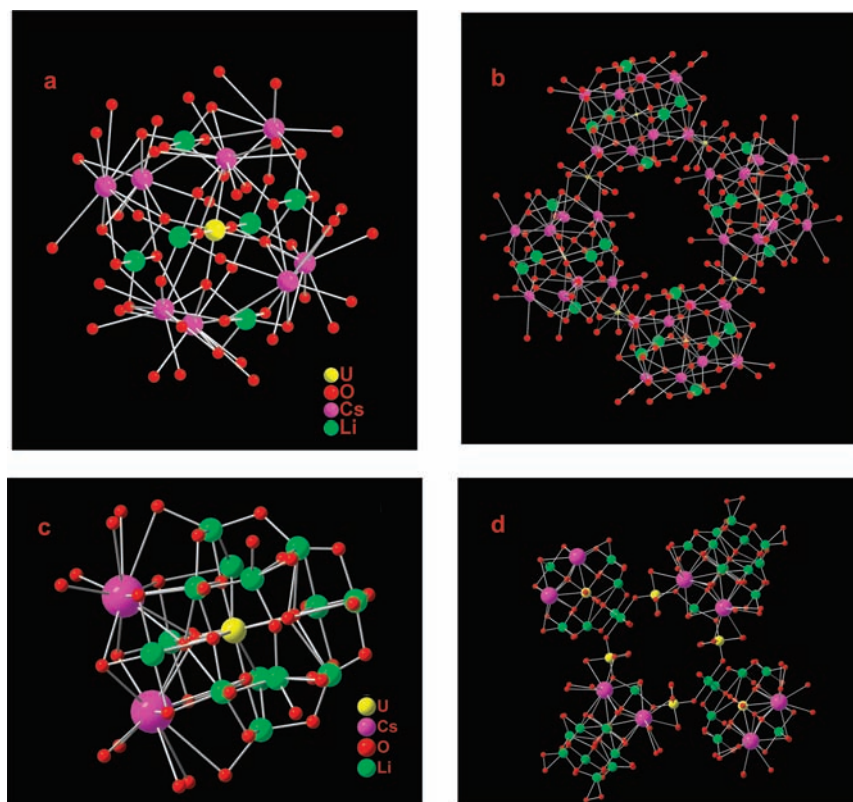


Figure 6. (a–b) Views of Cs-(2a). (a) the CsLi-UO₂(OH)₄ cluster, and (b) shows clusters linked into a ring by four UO₂(O₂)₃ anions. (c–d) Views of Cs-(2b). (c) the CsLi-UO₂(O₂)₃ cluster and (d) four of these clusters linked into a ring by four UO₂(O₂)₃ anions.

overlapping bands in the same region of the spectra of (1) and (2) are likely the analogous bonds, and also the U–OH bond of (2). As we expect, this region is more complex; broader with more overlapping bands for (2), since it has two chemically and crystallographically unique uranyl anions. The region from around 970–1500 cm⁻¹ is assigned to the Li–O bonds. We confirmed this from an IR spectrum of LiOH·H₂O, which features lithium in tetrahedral coordination, bonded to both water and OH ligands. Furthermore, we do not observe these bands in the spectrum of Na₄[UO₂(O₂)₃]·9H₂O that contains no lithium. Again, as we would expect, the more complex lattice of (2) has many more peaks in this region, as well.

Synthesis. Our initial synthetic experiments were of relatively low concentration of peroxide, LiOH, and uranyl nitrate, compared to those from which uranyl nanospheres charge-balanced with lithium cations were obtained (i.e., U₂₄—containing 24 UO₂(O₂)₃ polyhedra;¹⁶ designated Burns' synthesis). In the Burns' synthesis the LiOH, uranyl nitrate, and peroxide concentrations are respectively 4.5× greater, 3.7× greater, and 3× greater than for syntheses reported here. In addition to our initial syntheses, we prepared aqueous uranyl nitrate/LiOH/H₂O₂ solutions that were identical to those of the Burns' synthesis, and then

processed these solutions by both rapid addition and vapor diffusion of alcohol. The higher concentration Burns' solutions still gave (1) via rapid addition of alcohol, but a mixture of (1) and (2) via vapor diffusion of alcohol. These results were consistent, regardless of the alcohol (methanol, ethanol, or isopropanol). This suggests that crystallization of (1) and (2) rather than polynuclear clusters such as U₂₄ is a function of the alcohol–water media, rather than concentration of uranyl, base or peroxide. One might particularly expect higher uranyl concentration to favor the formation of a cluster such as U₂₄. Obtaining a mixture of (1) and (2) from alcohol diffusion into solutions with higher uranyl concentration is likely a function of crystallization rate. Alcohol diffusion into the lower uranyl concentration solutions gives only (2), and crystals are not observed until after 3–4 days of diffusion. On the other hand, crystals of (1) are visible after ~4 h, and both (1) and (2) are both apparent after 15 h of alcohol diffusion into the high uranyl concentration solution. The implication of these results is that crystallization of (2) requires more time for self-assembly. Although we repeatedly observe crystallization of (1), there are probably other lattice arrangements of hydrated Li⁺ and [UO₂(O₂)₃]⁴⁻. Finally, from the lower concentration solutions, pure phases of (1) and (2) were obtained, as observed in Figure 9,

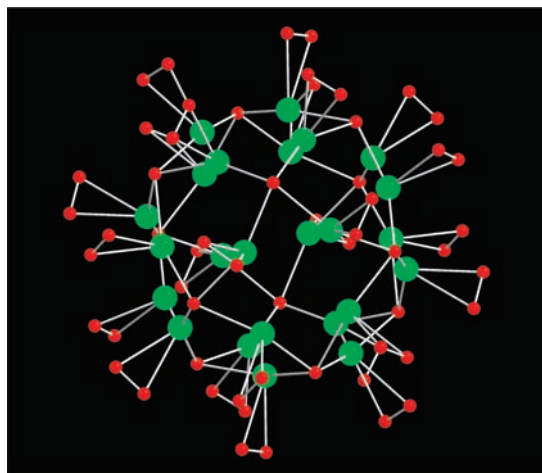


Figure 7. View of spherical arrangement of lithium-water-peroxide cluster, $\text{Li}_{24}(\text{H}_2\text{O})_{12}(\text{O}_2)_{24}$ observed in **Cs-(2a)**.

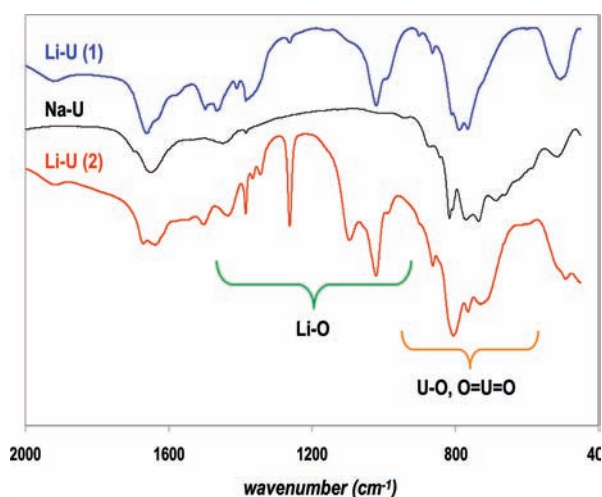


Figure 8. Infrared spectra of the two lithium salts **(1)** and **(2)**, along with $\text{Na}_4[\text{UO}_2(\text{O}_2)_3] \cdot 9\text{H}_2\text{O}^9$ (**Na-U**) for comparison. Vibrations for **Li-O** and **U=O** and **U-O** bonds are noted.

comparing the X-ray powder diffraction spectra of **(1)** and **(2)** to the calculated diffraction patterns from the single-crystal data.

In addition to the mixed **LiCs-U** and **LiRb-U** compounds, we also attempted to form a mixed **LiK-U** phase. Ethanol diffusion into the **Li-K-U** solution yielded **(2)**, with lithium only. Analogous solutions with only **Na**, **K**, **Rb**, or **Cs** produce different phases. Therefore it is really the **Li** that promotes the self-assembly of these clusters, but inclusion of the larger **Rb/Cs** in the clusters of **(2)** is driven by stronger ion-association behavior than that exhibited by **K**. Alcohol-water mixtures are less polar than aqueous solutions, which notoriously increases cation-anion pairing both in solution and in resulting precipitated phases.^{22–24} In particular for the introduction of alcohol via vapor-phase diffusion, we can surmise that the assembly of **(2)** in an alcohol-water media is the

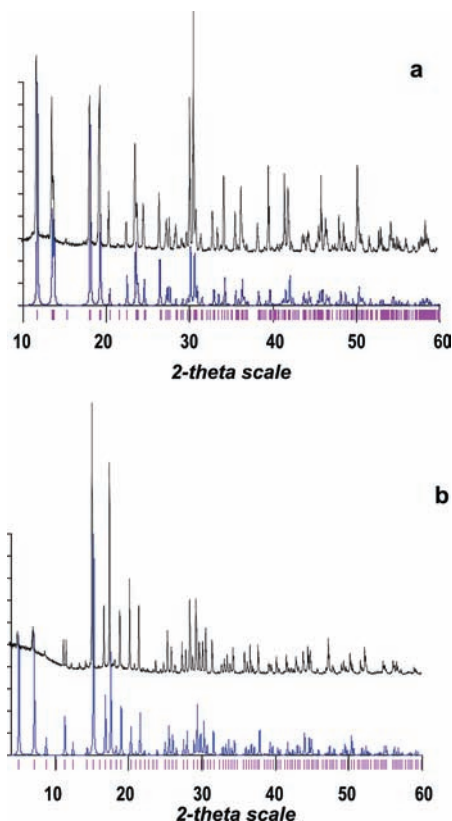


Figure 9. Powder X-ray diffraction spectra of **(1)** (top, **a**) and **(2)** (bottom, **b**): Experimental is the black trace, calculated from single crystal data is the blue trace, and the peak positions are the purple vertical marks.

result of contact ion-pairing between uranyl-peroxy and uranyl-hydroxyl anions and alkali cations. The pairing is described as contact-ion pairing because the lithium cations are bonded directly to the peroxide, hydroxyl, and oxo ligands of the uranium. This is a departure from the expected behavior: the small lithium cation generally carries a large hydration sphere, and thus its ion-pairing behavior tends to be solvent-mediated rather than by direct contact, both in solution and in precipitated phases. Water-mediated contact pairing between clusters and smaller cations (i.e., **Li**) contrasting direct bonding between clusters and larger cations (i.e., **Rb**, **Cs**) has been consistently observed in polyoxometalate systems.^{25–28} On the other hand, for crystallization of **(1)**, when the alcohol is introduced rapidly, the lithium cations retain their hydrated state and associate with the uranyl-peroxide anions only through H-bonding of the lithium-bound waters.

Summary and Conclusions

Two new structures of lithium uranyl-peroxide/hydroxyl salts have been obtained from alcohol-water solutions of uranyl nitrate, hydrogen peroxide, and lithium hydroxide. While one resembles previously reported $\text{Na}_4[\text{UO}_2(\text{O}_2)_3] \cdot x\text{H}_2\text{O}$ structures, the second has some unique features including (1)

(25) Antonio, M. R.; Nyman, M.; Anderson, T. M. *Angew. Chem., Int. Ed.* **2009**, *48*, 6136–6140.

(26) Grigoriev, V. A.; Hill, C. L.; Weinstock, I. A. *J. Am. Chem. Soc.* **2000**, *122*, 3544–3545.

(27) Grigoriev, V. A.; Cheng, D.; Hill, C. L.; Weinstock, I. A. *J. Am. Chem. Soc.* **2001**, *123*, 5292–5307.

(28) Nyman, M.; Alam, T. M.; Bonhomme, F.; Rodriguez, M. A.; Frazer, C. S.; Welk, M. E. *J. Cluster Sci.* **2006**, *17*, 197–219.

(22) Pigga, J. M.; Kistler, M. L.; Shew, C. Y.; Antonio, M. R.; Liu, T. B. *Angew. Chem., Int. Ed.* **2009**, *48*, 6538–6542.

(23) Chaumont, A.; Wipf, G. *Phys. Chem. Chem. Phys.* **2009**, *10*, 6940–6953.

(24) Marcus, Y.; Hefter, G. *Chem. Rev.* **2006**, *106*, 4585–4621.

two types of uranyl polyhedra, $\text{UO}_2(\text{O}_2)_3$ and $\text{UO}_2(\text{OH})_4$; and (2) direct bonding of lithium to the uranyl ligands, where lithium ions in salts crystallized from aqueous systems are usually bonded to water molecules. Furthermore the $\text{UO}_2(\text{OH})_4$ sits in the center of a polyoxometalate-like cluster with 1 uranyl polyhedron and 16 lithium polyhedra; and these clusters are linked together into rings and spheres via the $[\text{UO}_2(\text{O}_2)_3]^{4-}$ anions. Additionally, isostructural compounds with partial substitution of Cs or Rb into the alkali-uranyl clusters have been repeatedly obtained. The crystallization technique of vapor diffusion of alcohol into aqueous media provided an opportunity for this unusual self-assembly that appears to be guided by cation–anion association. The general strategy of induced self-assembly by slowly decreasing solvent polarity may be employed more generally in the uranyl-peroxide aqueous system with other cations such as transition metal complexes or lanthanides.

Finally, in general terms, the importance of alkali metals in aqueous polyanion metal systems is widely recognized. Alkali

metals control and mediate cluster assembly (geometry), dissolution, and crystallization, electron-transfer, anion–anion interactions, and super-assembly in solution and at interfaces. These studies provided fundamental information on the alkali–uranyl interactions in aqueous media.

Acknowledgment. This material is based upon work supported as part of the Materials Science of Actinides, an Energy Frontier Research Center funded by the U.S. Department of Energy, Office of Science, Office of Basic Energy Sciences under Award Number DE-SC0001089. Sandia is a multiprogram laboratory operated by Sandia Corporation, a Lockheed-Martin Company, for the United States Department of Energy under Contract No. DE-AC04-94AL85000.

Supporting Information Available: Crystallographic information files (cif) for (1), (2), Cs-(2a), and Cs-(2b). This material is available free of charge via the Internet at <http://pubs.acs.org>.